Emergence and stability of periodic two-cluster states for ensembles of excitable units

Robert Ronge* and Michael A. Zaks†
Institut für Physik, Humboldt-Universität zu Berlin, 12489 Berlin, Germany

(Received 14 October 2020; accepted 6 December 2020; published 7 January 2021)

We study dynamics in ensembles of identical excitable units with global repulsive interaction. Starting from active rotators with additional higher order Fourier modes in on-site dynamics, we observe, at sufficiently strong repulsive coupling, large-scale collective oscillations in which the elements form two separate clusters. Transitions from quiescence to clustered oscillations are caused by global bifurcations involving the unstable clustered steady states. For clusters of equal size, the scenarios evolve either through simultaneous formation of two heteroclinic trajectories or through two simultaneous saddle-node bifurcations on invariant circles. If the sizes of clusters differ, two global bifurcations are separated in the parameter space. Stability of clusters with respect to splitting perturbations depends on the kind of higher order corrections to on-site dynamics; we show that for periodic oscillations of two equal clusters the Watanabe-Strogatz integrability marks a change of stability. By extending our studies to ensembles of voltage-coupled Morris-Lecar neurons, we demonstrate that similar bifurcations and switches in stability occur also for more elaborate models in higher dimensions.

DOI: 10.1103/PhysRevE.103.012206

I. INTRODUCTION

Oscillatory states, ubiquitous in natural and artificial systems, are of particular interest when they emerge as collective phenomena through interactions in ensembles of smaller coupled units [1–3]. Depending on the individual dynamical properties of the ensemble constituents, three cases may be roughly distinguished: (a) the case where already in the absence of interaction every single unit is oscillating, treated, e.g., in the seminal paper of Kuramoto [4] and, under the assumption of weak coupling, reducible to a system of phase oscillators [5], (b) the case where without coupling some units oscillate on their own whereas the others are at rest [6,7], and (c) the case where all units stay at rest as long as they do not interact with each other but can show nontrivial collective dynamics if they interact [8].

Systems where every single unit is quiescent if isolated but may oscillate if "stimulated" in some appropriate way play a crucial role in neuroscience: A typical single neuron on its own is at rest, but a sufficiently strong input, e.g., in form of incoming action potentials from other neurons in a network, provokes *spikes* in its membrane voltage. This property, known as *excitability* [9], allows us to view the neuron as a dynamical system, close to some kind of limit cycle bifurcation [10]. In the course of the spike, a sufficiently large perturbation away from the stable state of rest rapidly grows before eventually converging back to rest, thereby tracing fragments of a hidden large-scale limit cycle. In particular, what is known as *class I excitability* [11] relates to the neuron being close to a saddle-node homoclinic bifurcation [12], also known as the saddle-node bifurcation on an invariant circle (SNIC). The scenario of this global codimension-1 bifurcation with normal form $\dot{x} = \varepsilon + x^2$, $x \in \mathbb{R} \cup \{\infty\}$ begins with negative value of the bifurcation parameter ε: the stable equilibrium at $-\sqrt{-\varepsilon}$ and the unstable one at $\sqrt{-\varepsilon}$ are connected by two orbits that start at the latter and end at the former. At $\varepsilon = 0$, two equilibria merge into a neutrally stable state of rest with a homoclinic trajectory (imagine x diverging toward $+\infty$ and "coming back" to the origin from $-\infty$) which for $\varepsilon > 0$ gives rise to a periodic orbit.

Probably the simplest example of a class I excitable unit is the *active rotator* [13] which obeys the Adler equation [14] $\dot{\phi} = \omega - \sin\phi$ for the variable ϕ. For $\omega^2 > 1$, ϕ rotates on the circle S^1. Here, e.g., $\varepsilon = |\omega| - 1$ can serve as a bifurcation parameter for the two SNIC at $\omega = \pm 1$.

Coming back to the general classification of ensembles of potentially oscillating units in terms of neuroscience vocabulary, the first two cases of ensemble dynamics listed in the opening paragraph may be referred to as pure ensembles of oscillating units or mixed ensembles of oscillating and excitable units while the third case regards pure ensembles of excitable units.

While there is a large body of literature for the first two cases, less attention has been paid to ensembles of exclusively excitable units, perhaps because many contexts favor attractively coupled elements. Let us informally separate two types of coupling. Whenever two units are put at a close distance and the action of the coupling between them tends, regardless of the position in the phase space, to *decrease* this distance, we call the coupling between these units *attractive*. If, on the contrary, the coupling between two close units, regardless of their position, contributes to the *increase* of the distance between them, we call the coupling *repulsive*. Below, we consider the interactions that vanish when the states of interacting elements exactly coincide.

Attractive coupling for excitable units leads to trivial behavior. Each decoupled unit, if perturbed, eventually converges to its stable state of rest. Attractive coupling (for identical elements) only makes this tendency collective.

*robert.ronge@physik.hu-berlin.de
†michael.zaks@physik.hu-berlin.de

Hence, nontrivial dynamics for ensembles of excitable units needs at least some of the units to be coupled repulsively [15].

Below, we restrict ourselves to ensembles of identical units. If, in the absence of coupling, each element possesses the unique robust stable state of rest, the synchronous collective equilibrium with every unit at the rest position exists and remains stable as long as repulsion is weak. Recently, a scenario of destabilization of this state of rest for the case of identical all-to-all repulsively coupled active rotators was discussed [8]. One of the main results was the existence, for sufficiently strong repulsive coupling, of the continuous family of periodic solutions with neutral stability where different initial conditions lead to different asymptotic periodic states. This neutral stability has to do with the fact that the model, treated in [8] and based on sinusoidally coupled active rotators [13], features what is known as the Watanabe-Strogatz (WS) integrability [16]. The latter phenomenon holds for a set of N identical phase variables that obeys a fairly general set of conditions [17]. It leads to highly degenerate dynamics, caused by foliation of the phase space in invariant three-dimensional manifolds and goes along with the existence of $N-3$ conserved quantities. At least for N large enough, the WS formalism shows that this continuum of periodic states emerges exactly when one of the synchronous states of rest changes its stability under sufficiently strong repulsive coupling [18]. Since neutral stability is a strong hint that a periodic solution is not persistent under perturbations of the vector field, the question arises of how common this family of periodic orbits really is. To investigate more persistent scenarios of transition from rest to collective oscillations is the main objective of the current paper.

It turns out that there exists another type of periodic oscillations that, in the course of enhancement of the repulsive coupling, emerges independently from the WS-related family of periodic orbits. This type of solution is a state where the ensemble splits in two groups, inside which all units assume the same instantaneous values: a two-cluster state. In this work, we investigate through which bifurcation scenarios these periodic states emerge and how their stability is affected by higher order Fourier modes in their on-site dynamics.

Dynamics of clustered states has been thoroughly studied in the context of phase oscillators and in other similar setups. In particular, formation of two clusters of equal or comparable size has been encountered in many different contexts, from neuroscience to electrochemistry [19–23]. Below, we extend those studies to the case, when the uncoupled units do not oscillate, and the very existence of oscillating clusters owes to the interaction between the elements. It turns out that in the WS dynamics the oscillatory states composed of two oscillating clusters play a special role, different from those of other periodic solutions.

This paper is divided in two parts. In Sec. II, we present the ensemble of active rotators (II A) and our results concerning the existence and stability of two-cluster solutions. Starting in Sec. II C with a reduced (two-dimensional) description in terms of cluster coordinates, we discuss in Secs. II D and II E the global bifurcation scenarios, observed within this reduced model for clusters of equal or unequal size at different choices of system parameters, and complete our discussion in Sec. II F by numerical stability analysis of collective oscillations. In Sec. III, we go beyond active rotators and consider an ensemble of two-dimensional excitable units of Morris-Lecar neurons [24]. This is a common choice for systems of mixed ensembles [6,7] because its parameters can be tuned to ensure class I excitability or oscillatory behavior [25,26]. We briefly discuss emergence and stability of periodic two-cluster states in this system and how the results for the phase model translate to ensembles of more general excitable elements.

II. COUPLED ACTIVE ROTATORS

A. The model

We start by discussing the active rotator model and basic properties of observed two-cluster periodic solutions.

Consider the system $\dot{\phi} = f(\phi, \delta)$ for a phase-like[1] variable $\phi \in S^1$ with the bifurcation parameter δ in some open interval around 0, and assume that for $\delta < 0$ the function f possesses exactly two regular zeros $f(\phi^s, \delta) = f(\phi^u, \delta) = 0$ with $f'(\phi^s, \delta) < 0$ and $f'(\phi^u, \delta) > 0$, and no zeros whatsoever for $\delta > 0$ (f' denotes the derivative of f with regard to ϕ). The zero point ϕ^s is then the stable equilibrium of the system and ϕ^u is the unstable one. At $\delta = 0$ the system undergoes a saddle-node bifurcation on the invariant circle S^1. (Interested in class I excitability, we always implicitly assume that $\delta < 0$ is chosen such that two zeros ϕ^s and ϕ^u lie "close enough" to each other on the circle.) We call this system an *active rotator*.

If the function $g : S^1 \to \mathbb{R}$ has a regular zero at zero argument, we call it an *attractive* coupling function if $g'(0) < 0$ and a *repulsive* coupling function if $g'(0) > 0$.

We are interested in systems of N identical active rotators which we assume to be coupled in such a way that the interaction (i) is pairwise, (ii) depends on the difference between the phases, (iii) is all to all, and (iv) is repulsive. Such a system can be written as

$$\dot{\phi}_j = f(\phi_j, \delta) + \frac{1}{N}\sum_{k=1}^{N} g(\phi_k - \phi_j),$$

with $f(\phi, \delta)$ describing the "internal" (on-site) dynamics of each phase variable and g being the coupling function between any pair of phases. Cyclic nature of the phase implies 2π periodicity of f and g with respect to phase arguments. The phase space is a torus $T^N := S^1 \times \cdots \times S^1$ of dimension N. Notably, phases cannot surpass each other; in other words, for a lift of the system from T^N to $\mathbb{R}^N$, a fixed order of phases, say $\phi_1 \leqslant \phi_2 \leqslant \cdots \leqslant \phi_N < \phi_1 + 2\pi$ at some time t leads to the same order at any other time t'. Equivalently, $\phi_j(t_0) = \phi_k(t_0)$ at time t_0 implies $\phi_j(t) = \phi_k(t)$ for all t.

The arguably simplest model of this type, introduced by Shinomoto and Kuramoto [13], is of the form

$$\dot{\phi}_j = \omega - \sin\phi_j + \frac{\kappa}{N}\sum_{k=1}^{N} \sin(\phi_k - \phi_j),$$

where for each isolated unit j, a SNIC occurs at $\omega = \pm 1$ and the coupling is repulsive if $\kappa < 0$. Each unit is an active rotator

[1]Below, we use the term "phase" in the colloquial sense: unlike a proper phase, ϕ does not rotate uniformly; moreover, for a nonoscillatory system the proper phase cannot be introduced.

if $|\omega| < 1$ so that $|\omega| - 1$ may serve as the bifurcation parameter δ. Publications on variants of this model, mostly involving action of noise, include Refs. [27–29] as well as Ref. [8]. Since the model fulfils provisions of the Watanabe-Strogatz integrability (identical units are coupled to the common field only via their first Fourier modes), the class of possible attractors is immensely reduced [30]. Therefore, to account for more generic kinds of ensemble dynamics, the system should be modified; a natural way to do this is to take into account higher Fourier modes. Below, we violate the WS condition by including the higher modes in the on-site part $f(\phi_j)$ of

$$\dot{\phi}_j = f(\phi_j) + \frac{\kappa}{N}\sum_{k=1}^{N}\sin(\phi_k - \phi_j). \tag{1}$$

On introducing

$$V(\phi_1,\ldots,\phi_N) = -\sum_k \int f(\phi_k)\,d\phi_k - \frac{\kappa}{2N}\sum_{j,k}\cos(\phi_k - \phi_j),$$

we observe that regardless of the particularities of $f(\phi)$, dynamics of the system (1) is of the gradient type: $\dot{\phi}_j = -\partial V/\partial\phi_j$. This property [shared by arbitrary odd coupling functions $g(-\xi) = -g(\xi)$] prohibits small-scale periodic motions and, as a consequence, the Hopf bifurcations. Hence, emergence of periodic states occurs only through global bifurcation scenarios.

In the space of all periodic $f(\phi)$, the WS case—absence of all higher Fourier harmonics—has infinite codimension, and does not occur in generic families with finite number of parameters (like Hamiltonian dynamics does not occur in generic families of ordinary differential equations). However, at our starting point—the rotators of Refs. [13] and [8]—this degeneracy is ensured by design, and therefore we consider below specially tailored families of functions for which simultaneous vanishing of all higher order terms becomes the codimension-1 event. Choosing appropriate rescaling and shift of the variables ϕ_j and time t, we rewrite local dynamics as

$$f(\phi) = \omega - \sin\phi + \epsilon\sum_{n=2}^{\infty}\left(c_n e^{in\phi} + \bar{c}_n e^{-in\phi}\right), \tag{2}$$

separating the higher order Fourier terms from the zeroth- and first-order terms. Here, $\bar{z}$ denotes the complex conjugate of a complex number z, and the new parameter ϵ controls the deviation from the WS case (i.e., $\epsilon = 0$).

To make the problem more definite, we consider two exemplary cases of local dynamics:

$$f(\phi) = \omega - \sin\phi + \epsilon\sin 2\phi, \tag{3a}$$

$$f(\phi) = \omega - \sin\phi + \epsilon\left(\frac{1}{\sin\phi - 2} + a + b\sin\phi\right). \tag{3b}$$

The case (3a) where merely the second Fourier harmonic is added is a simple way to perturb the original system; it allows for explicit expressions for certain bifurcations (see below). The case (3b) features infinitely many Fourier harmonics and is a representative of more common "perturbations" away from the WS-integrable system of Ref. [8]. The Fourier expansion of the perturbative term in (3b) reads

$$\left(a - \frac{1}{\sqrt{3}}\right) + \left(2 - \frac{4}{\sqrt{3}} + b\right)\sin\phi - \left(8 - \frac{14}{\sqrt{3}}\right)\cos 2\phi + \cdots.$$

Below we fix $a = 1/\sqrt{3}$ and $b = 4/\sqrt{3} - 2$, so that the two first terms in the expansion vanish and the deviation from the Shinomoto-Kuramoto form starts from the second Fourier harmonics. With both perturbations in (3a) and (3b) bounded by $\pm\epsilon$, the function f at $|\omega| < 1$ and sufficiently small $|\epsilon|$ still possesses two regular zeros nearby, so that both cases indeed describe an active rotator.

Since all units are identical, their arbitrary permutations for a periodic state trivially yield different periodic states. Therefore, we henceforth assume the units to be in a natural order $\phi_1 \leqslant \phi_2 \leqslant \cdots \leqslant \phi_N < \phi_1 + 2\pi$.

Integrating Eq. (1) numerically for different choices of f reveals various kinds of periodic attractors. Among them, two types play the prominent role. The first one includes splay states: periodic solutions of the form $\phi_j(t) = \phi(t + \frac{j}{N}T)$, $j = 0,\ldots,N-1$ for some T-periodic function $\phi(t)$. There, the consecutive units j and $j+1$ are always separated by the time interval T/N in their respective dynamics. The other type is a two-cluster periodic solution: The ensemble is composed of two groups of oscillating units within which the instantaneous states coincide. We will discuss the properties of splay states elsewhere [18] and concentrate here on the origin and properties of the two-cluster solutions.

Besides these two, there can be other, possibly stable, periodic solutions. Among them is kind of a combination of both types: the clustered splay states where the ensemble splits in a set of clusters that are regularly staggered in time. Further, if the clusters are not of the same size, this staggering is, at best, approximate. It seems that these states emerge in the same way as the true splay state. Yet other periodic states can exist but in our simulations the majority of initial conditions has lead to either two-cluster states or (clustered) splay states. This is why we focus on these two types.

Both choices for $f(\phi)$ characterize on-site dynamics in terms of two parameters ω and ϵ. Together with the coupling strength κ, this yields a three-parameter description. Being interested in the coupling-induced effects, below we largely discuss the scenarios that evolve when $|\kappa|$ is increased and plot slices of the parameter space along the planes of constant ω.

A notable difference between a Kuramoto phase oscillator and an active rotator is the homogeneous evolution of the phase for the former and the coordinate-dependent $d\phi/dt$ for the latter. As a result, in case of the global coupling the symmetry of the ensemble of identical phase oscillators is higher than of the ensemble of identical active rotators: Both ensembles share the richness of permutation symmetries, but dynamics of the former is invariant with respect to the simultaneous shift of all phases by an arbitrary constant, whereas the latter ensemble lacks this invariance. This may contribute to the absence of persistent heteroclinic networks, characteristic for phase oscillators with higher order Fourier terms [19,31,32], in our numerical simulations of the ensembles of

active rotators. Instead, as demonstrated below, introduction of the higher order harmonics leads to the expected destruction of the WS continuum of periodic orbits and to the birth of collective oscillations via the formation of structurally unstable saddle connections.

B. Destabilization of the synchronous equilibrium

In the absence of coupling, the ensemble of active rotators (1) possesses a unique simple attractor: the synchronous steady state Φ^s, with every unit at its stable state of rest ϕ^s. The value ϕ^s, entirely prescribed by on-site dynamics, is independent of the coupling κ. Growth of the repulsion intensity gradually weakens stability of this collective equilibrium, until, at a threshold negative value of κ, its destabilization occurs. Permutation symmetry of the units turns the latter into the global event: a *transcritical heteroclinic* bifurcation [8,33,34]. For the on-site dynamics of the type (3a), the critical values of the parameters κ, ω, ϵ are interrelated[2] by

$$\begin{aligned}&\kappa^2+\omega^2+12\epsilon^2-48\epsilon^4+64\epsilon^6+4\epsilon^2\kappa^2\\&-32\epsilon^4\kappa^2-4\epsilon\kappa^3+4\epsilon^2\kappa^4-80\epsilon^2\omega^2\\&+64\epsilon^2\omega^4-128\epsilon^4\omega^2+32\epsilon^2\kappa^2\omega^2=1.\end{aligned}\tag{4}$$

At small values of $|\epsilon|$ this translates to the explicit expression for the critical coupling intensity:

$$\kappa_0=-\sqrt{1-\omega^2}+2\epsilon(1-\omega^2)+2\epsilon^2\omega^2\frac{4\omega^2-5}{\sqrt{1-\omega^2}}+O(\epsilon^3).\tag{5}$$

As described in Ref. [8], destabilization of the synchronous equilibrium is a highly degenerate event: $N-1$ Jacobian eigenvalues simultaneously vanish. At the moment of bifurcation, $\sim 2^{N-1}$ steady states coalesce with the synchronous equilibrium. For the overwhelming majority of them, the bifurcation is transcritical. There is, however, one important exception: The clustered steady states in which the ensemble splits into two *equal* groups, branching off the synchronous steady state via a pitchfork bifurcation. Depending on the values of ω and ϵ, this pitchfork can be super- or subcritical; see Fig. 1. As derived in Appendix B, for the local dynamics of the kind (3a) at not too big $|\epsilon|$, the pitchfork is subcritical if the quantity

$$c=\frac{(\sin\phi^s-4\epsilon\sin 2\phi^s)^2}{\cos\phi^s(\cos\phi^s-2\epsilon\,\cos 2\phi^s)}$$

exceeds 1. If $c<1$, the pitchfork is supercritical.

Change of the pitchfork character is a codimension-2 bifurcation that in the space, spanned by ϵ, ω, κ, happens on a one-dimensional set. It is convenient to parametrize it, e.g., in terms of ϵ: The corresponding value of $\omega(\epsilon)$ is found from

$$\begin{aligned}&4(1-2\omega^2)^2-\epsilon^2(48-545\omega^2+1924\omega^4-1796\omega^6)\\&+4\epsilon^4(48-1393\omega^2+9390\omega^4-22272\omega^6+16384\omega^8)\\&-4\epsilon^6(64-273\omega^2+256\omega^4)=0.\end{aligned}\tag{6}$$

[2]Derivation of Eqs. (4) and (6) and similar expressions is briefly explained in Appendix A.

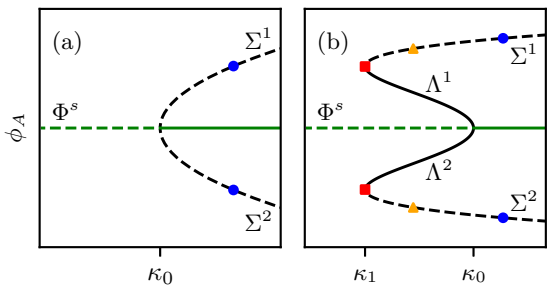

FIG. 1. Variants of the pitchfork bifurcation involving the synchronous state of rest Φ^s and steady states, built by two equal clusters. Solid curves, stable steady states; dashed curves, unstable ones. Left panel: subcritical pitchfork at κ_0. Global bifurcations involving the saddles Σ^i ($i=1,2$; cf. Sec. II D) can only occur for $\kappa \geqslant \kappa_0$ (blue disks). Right panel: supercritical pitchfork at κ_0. New stable steady states Λ^i branch off Φ^s at κ_0 and vanish at κ_1 in simultaneous saddle-node bifurcations with Σ^i. Here, the periodic two-cluster orbit is born in either of two possible ways. In the first scenario, it is created in the double heteroclinic bifurcation for some $\kappa_{\rm het} \geqslant \kappa_1$. There is a hysteresis: at $\kappa_{\rm het} \geqslant \kappa_0$ (blue disks) with the stable Φ^s, and at $\kappa_1 < \kappa_{\rm het} \leqslant \kappa_0$ (orange triangles) with the stable Λ^i. Basins of attraction are separated by separatrices of the saddles Σ^i. In the second scenario, the periodic orbit comes into existence at κ_1 via a double SNIC (red squares).

[Equally, one can parametrize the curve by ω and solve the same equation for $\epsilon(\omega)$.] Finally, the value of $\kappa(\epsilon, \omega(\epsilon))$ on the curve is recovered from Eq. (4). Along this curve in the parameter space, the two-dimensional surface of saddle-node bifurcation branches off the two-dimensional surface (4) of the pitchfork bifurcation.

C. Reduced description

Since identical units group as a cluster in finite time only if they are initialized as one, it is reasonable to consider a reduced (i.e., two-dimensional) model. We order the ensemble in such a way that the first pN units have equal phase, as have the remaining $(1-p)N$ ones; here $p \in \{0, 1/N, 2/N, \ldots, 1\}$ is the proportion of cluster A and $(1-p)$ is the proportion of cluster B. We introduce the cluster coordinates $\phi_A(t)$ and $\phi_B(t)$ that obey

$$\begin{aligned}\dot\phi_A&=f(\phi_A)+(1-p)\,\kappa\,\sin(\phi_B-\phi_A),\\\dot\phi_B&=f(\phi_B)-p\,\kappa\,\sin(\phi_B-\phi_A),\end{aligned}\tag{7}$$

since units within the same cluster do not interact. If the ensemble forms two clusters of unequal size (i.e., $p \neq \frac{1}{2}$), we deal thus with a system of two nonidentical units that both repel each other; this setup close to a SNIC bifurcation was investigated in a more general setting under the assumption of weak coupling in Ref. [35]. The phase space of the reduced system (7) is a 2-torus.

It is noteworthy that each value of p defines a different invariant subspace in the phase space of the full system. Every value of p prescribes how many units belong to each cluster so that any two subspaces with different values of p intersect only along the line of complete synchrony (one-cluster state),

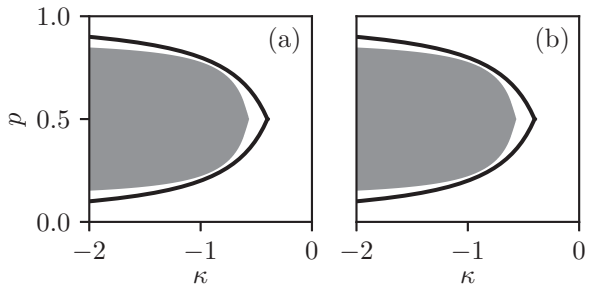

FIG. 2. Existence of periodic two-cluster solutions of (1) in dependence on κ and p at fixed $\omega = 0.8$ and $\epsilon = 0.1$ for two choices of f. (a) On-site dynamics of the type (3a). (b) On-site dynamics of the type (3b). Dark shading: existence of the periodic two-cluster state with the cluster A of size pN and the cluster B of size $(1-p)N$. In the white region, no periodic two-cluster solutions exist. Black curves: approximate bounds on p for the existence of periodic two-cluster states of size ratio $\frac{p}{1-p}$, given by Eqs. (10) and (11).

$\phi_A = \phi_B$. This observation becomes useful in the discussion of bifurcation scenarios in Sec. II D.

Two-cluster states of rest of Eq. (1) are solutions of Eq. (7) with vanishing time derivatives. For each of them, Np coordinates assume the value ϕ_A whereas $N(1-p)$ coordinates are equal to ϕ_B. Due to coincidence of the values, the spectrum of the Jacobian matrix at these states is highly degenerate [36]. Along with two simple eigenvalues $\lambda^+ > 0$ and $\lambda^- < 0$, obtained from the linearization of (7) at the point (ϕ_A, ϕ_B), there is the eigenvalue

$$\lambda^A = f'(\phi_A) - \kappa(p + (1-p)\cos(\phi_A - \phi_B)) \tag{8}$$

with multiplicity $Np - 1$, as well as the eigenvalue

$$\lambda^B = f'(\phi_B) - \kappa(1 - p + p\cos(\phi_A - \phi_B)) \tag{9}$$

with multiplicity $N(1-p) - 1$.

In the eigenspaces corresponding to λ^A and λ^B, we choose a basis $\{e^j\}_{j=2,\ldots,Np}$ of the form $e_i^j = \delta_{j,i} - \delta_{1,i}$ and $\{e^j\}_{j=Np+2,\ldots,N}$ with $e_i^j = \delta_{j,i} - \delta_{Np+1,i}$ ($\delta_{i,j}$ being the Kronecker delta). Thereby, a perturbation along each vector in these eigenspaces leaves one cluster intact but kicks units off from the other cluster.

On the other hand, one-dimensional eigenspaces for $\lambda^\pm$ are of the form $e^\pm = (a, \ldots, a, b, \ldots, b)$ with $a \neq b$, so that the first Np entries are equal, as are the last $N(1-p)$ ones. Hence, along these eigenspaces the clusters stay whole. Therefore, we call the eigenspaces either *splitting* (for λ^A and λ^B) or *nonsplitting* (for λ^+ and λ^-). Splitting of clusters can be a source of highly nontrivial dynamical effects; see, e.g., Refs. [19,31,37].

Proceeding from steady to oscillatory states, a natural question is which choices of parameters $(\omega, \epsilon, \kappa, p)$ enable existence of periodic two-cluster solutions. Since ω and ϵ only decide whether the units are active rotators or not, we fix them and determine the existence of two-cluster states in dependence on κ and p; this is equivalent to the existence of periodic solutions in the parameter space of the reduced system (7). Figure 2 shows the existence regions for $\omega = 0.8$, $\epsilon = 0.1$, and two kinds of f. Other choices for ω, ϵ, or the perturbation type lead to similar results.

Depending on the coupling strength κ, only those periodic two-cluster orbits can exist that are sufficiently balanced in size. In general, the more repulsive the coupling (i.e., the larger $|\kappa|$), the more the two oscillating clusters can differ in size. This is reasonable: For weaker coupling, the influence of the smaller cluster A on the larger one B wanes so that the latter, as if isolated, converges approximately to its single unit state of rest. Unable to overpass B, A cannot perform a large-scale oscillation either. This observation prompts a rough estimate on the lower and upper bounds for the values of p that, at $|\epsilon| \ll 1$, enable periodic states. Consider the general case of $f(\phi_j, \epsilon) = \omega - \sin\phi_j + \epsilon h(\phi_j)$ and $p < \frac{1}{2}$, which implies that cluster B is the larger one. Without loss of generality, let $\omega \geqslant 0$. We view the smaller cluster ϕ_A as a time-dependent perturbation of the isolated dynamics in the large cluster: $\dot{\phi}_B = f(\phi_b, \epsilon) + p\kappa\, g(t)$. The strongest repulsion between the clusters occurs at $\phi_A - \phi_B = \pm\pi/2$ so that the influence of ϕ_A upon ϕ_B is bounded by $\pm p\kappa$, which yields

$$\dot{\phi}_B \geqslant \omega - \sin\phi_B + \epsilon h(\phi_B) - p\kappa.$$

Hence, the flow of ϕ_B must possess a stable fixed point ϕ_B^* if the right-hand side of this equation has a zero in ϕ_B. For small $|\epsilon|$, this implies a lower boundary at $\omega - p\kappa \approx 1$. From this, we conclude that for the existence of periodic two-cluster states with size ratio $\frac{p}{1-p}$

$$p_{\min} \approx -\frac{1-\omega}{\kappa} \tag{10}$$

is a lower bound in p. Similarly, the upper bound is

$$p_{\max} \approx 1 + \frac{1-\omega}{\kappa}. \tag{11}$$

In Fig. 2, these bounds are plotted as black curves, along with the actual domain of existence of the periodic states.

D. Heteroclinic bifurcation scenarios

1. General considerations

We begin with the case $p = 1/2$ (and therefore implicitly assume N to be even[3]) not only while this choice is the simplest, but also due to the empirical observation: In our numerical simulations, two-cluster states with p far off the value $1/2$ have been rarely encountered as asymptotic attractors for random initial conditions. As discussed in the next section, for $p \neq 1/2$ the scenarios are not much different, because every invariant two-cluster subspace offers the same types of saddles. We start at $\kappa = 0$ where the interaction is formally absent and the ensemble consists of uncoupled units. On denoting the stable and unstable equilibrium of a single active rotator by ϕ^s and ϕ^u, respectively, the ensemble has altogether 2^N collective equilibria with each coordinate being either ϕ^s or ϕ^u. Fixing, without loss of generality, the ordering of phases $\phi_1 \leqslant \cdots \leqslant \phi_N < \phi_1 + 2\pi$, leaves two symmetric two-cluster steady states $\Sigma^1 = (\phi^s, \ldots, \phi^s, \phi^u, \ldots, \phi^u)$ and

[3]At the values of ω, ϵ, κ ensuring two stable equal clusters for even N, simulations with close odd values of N mostly end up with two equal oscillating clusters and a solitary element.

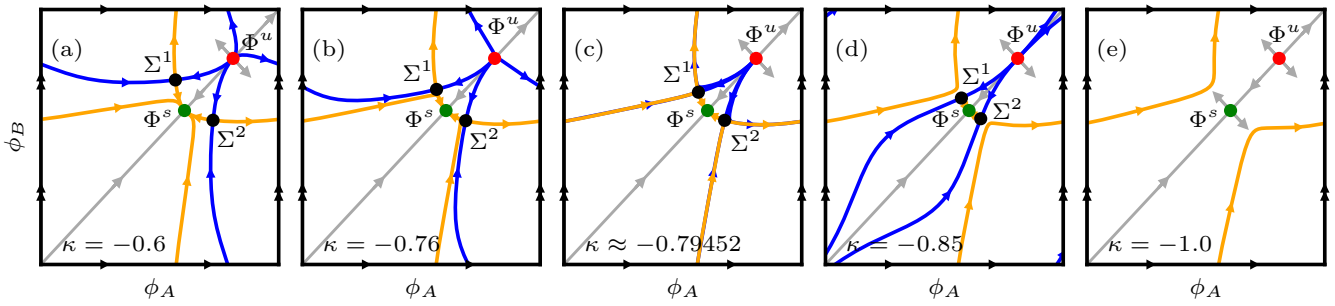

FIG. 3. Scenario of double heteroclinic bifurcation, creating a periodic two-cluster state (ϕ_A, ϕ_B) at $p = 1/2$, $\omega = 0.8$, and $\epsilon = -0.2$ for on-site dynamics of the type (3a). Here and in further figures, black arrows delimit domain of periodicity for the unfolding of the toroidal two-cluster subspace on the plane. In panel (a), at small $|\kappa|$, two synchronous steady states Φ^s (green disk) and Φ^u (red disk) coexist with two saddles $\Sigma^{1,2}$ (black disks). Each saddle is connected to Φ^s via two components of its unstable manifold $U(\Sigma^{1,2})$ (orange curves). Components of the stable manifolds of $\Sigma^{1,2}$ (blue curves) start at Φ^u. Invariant diagonal together with local invariant manifolds of Φ^s and Φ^u are marked in gray. (b) Decreasing κ lets $U(\Sigma^{1,2})$, on their way from $\Sigma^{1,2}$ to Φ^s, approach the opposite saddle $\Sigma^{2,1}$. (c) The incoming and outgoing separatrices of counterpart saddles merge in a simultaneous heteroclinic bifurcation. (d) The resulting invariant curve detaches from the saddles and becomes a periodic two-cluster state, stable with respect to non-splitting perturbations. (e) Finally, both saddles disappear in the course of a subcritical pitchfork bifurcation with Φ^s.

$\Sigma^2 = (\phi^u, \ldots, \phi^u, \phi^s, \ldots, \phi^s)$, where the first $N/2$ phases and the last $N/2$ ones form distinct clusters A and B.

Since the periodic two-cluster orbits must emerge through a global bifurcation and form by definition cluster states, it is reasonable to inspect dynamics in the reduced system (7). Reminiscent of a single excitable unit, observed bifurcation scenarios always involve a set of two-cluster equilibria on an invariant curve.

At $\kappa = 0$, the reduced system possesses four equilibria: a stable and an unstable synchronous points $\Phi^s = (\phi^s, \phi^s)$ and $\Phi^u = (\phi^u, \phi^u)$, as well as two saddles $\Sigma^1 = (\phi^s, \phi^u)$ and $\Sigma^2 = (\phi^u, \phi^s)$ (which we may, in an abuse of notation, identify with the steady states of the full system). Since in this uncoupled case each coordinate of the state $\phi = (\phi_A, \phi_B)$ represents a class I excitable unit, the toroidal phase space contains a contour C: the union of one-dimensional unstable manifolds $U(\Sigma^1)$ and $U(\Sigma^2)$ of the saddles Σ^1 and Σ^2. Naturally, Φ^s lies in C at the intersection of $U(\Sigma^1)$ with $U(\Sigma^2)$ so that C is shaped like a figure eight. This contour is robust under sufficiently small changes in κ since for $\kappa = 0$ is forms a normally hyperbolic invariant manifold [38] and so is preserved in the case of (weakly) coupled clusters A and B. In fact, numerical results confirm its persistence for fairly large $|\kappa|$. The contour C is a natural building block for the emergence of periodic two-cluster states.

For the synchronous state of rest Φ^s, stable for sufficiently small $|\kappa|$, the invariant diagonal $\phi_A = \phi_B$ is tangent to the stable eigenvector (1,1) of the Jacobian at Φ^s. In the normal direction, Φ^s eventually undergoes a pitchfork bifurcation, discussed above. Whether the latter is sub- or supercritical can have implications on how a periodic state forms from C since a supercritical pitchfork creates new equilibria that may interact with C (Fig. 1).

2. *Birth of periodic orbit from double heteroclinic connection*

For a detailed discussion of the bifurcation scenarios, we restrict ourselves to the local dynamics governed by Eq. (3a). Figure 3 shows, from left to right, a typical bifurcation scenario for the case when the pitchfork bifurcation of Φ^s is subcritical. On-site parameters are $\omega = 0.8$ and $\epsilon = -0.2$. On the torus, at moderate repulsive coupling κ [Fig. 3(a)], the unstable manifolds $U(\Sigma^{1,2})$ of the saddles, shown by orange curves, lead from $\Sigma^{1,2}$ to Φ^s. Additionally, the unstable node Φ^u is connected to the saddles $\Sigma^{1,2}$ by the components of their stable manifolds (blue curves). As repulsion increases, the curves $U(\Sigma^{1,2})$ come closer to the stable manifolds of the counterpart saddles [Fig. 3(b)], and merge with them, simultaneously forming two heteroclinic connections between $\Sigma^{1,2}$ [Fig. 3(c)]. Their subsequent breakup leaves the global smooth invariant curve: the periodic two-cluster state [Fig. 3(d)]. Its stability within the reduced subspace is decided in the competition between expansion and contraction near the saddles: by the ratio $|\lambda^-/\lambda^+|$ at the bifurcation [12]. According to our numerics, $|\lambda^-| > \lambda^+$: Contraction prevails, and hence the orbit is stable. We note that in terms of the reduced system of two cluster coordinates, this double heteroclinic bifurcation corresponds to the T point in Fig. 16 of Ref. [35]. At this stage of the scenario, the system is bistable; basins of attraction of the newborn periodic orbit and the still stable synchronous state of rest Φ^s are separated by separatrices of the saddles $\Sigma^{1,2}$. Finally, the saddles merge with Φ^s in the subcritical pitchfork bifurcation [Fig. 3(e)], and the periodic orbit remains the only attractor.

3. *The double SNIC bifurcation*

As seen in the panels of Fig. 1, the locus of the double heteroclinic bifurcation can, depending on the values of ω and ϵ, wander along the saddle branches of the bifurcation diagram. In the case of the subcritical pitchfork bifurcation, this wandering may end on the turning points of the diagram in Fig. 1(b): at the saddle-node bifurcation of steady states in the reduced system. This codimension-2 event is known as the *orbit flip* [12]: change of the direction from which a separatrix approaches the saddle. In terms of global dynamics, birth of the clustered periodic solution from the double heteroclinic bifurcation gets replaced by its birth from the

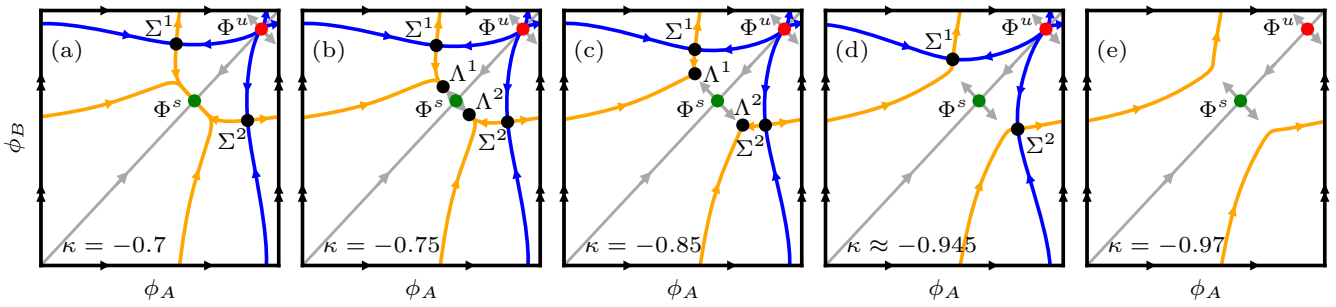

FIG. 4. Double SNIC bifurcation, producing a periodic two-cluster state (ϕ_A, ϕ_B) at $p = 1/2$, $\omega = 0.6$, and $\epsilon = 0.2$ for on-site dynamics of the type (3a). (a) At small $|\kappa|$, two synchronous steady states Φ^s (green disk) and Φ^u (red disk) coexist with two saddles $\Sigma^{1,2}$ (black disks). Each saddle is connected with Φ^s via two components of its unstable manifold (orange curves). Components of the stable manifolds of $\Sigma^{1,2}$ start at Φ^u (blue curves). Invariant diagonal together with local invariant manifolds of Φ^s and Φ^u are marked in gray. (b) Decreasing κ leads to the supercritical pitchfork bifurcation of Φ^s in which two new stable equilibria $\Lambda^{1,2}$ (black disks) appear. $\Sigma^{1,2}$ are connected with $\Lambda^{1,2}$ by their unstable manifolds. (c) In the course of the further decrease of κ, $\Lambda^{1,2}$ approach $\Sigma^{1,2}$. (d) Four states of rest undergo a simultaneous SNIC, leaving (e) in the phase space a periodic orbit as the only attractor.

double SNIC bifurcation. The latter bifurcation scenario, to our knowledge, has not been so far discussed in the context of collective oscillations of repulsively coupled excitable units.

Figure 4 sketches how, at fixed $\omega = 0.6$ and $\epsilon = 0.2$, the periodic two-cluster orbit forms after the supercritical pitchfork of Φ^s. Initially, in Fig. 4(a), two saddles $\Sigma^{1,2}$ are connected with their respective stable manifolds (blue curves) to the unstable synchronous steady state Φ^u and with their unstable manifolds (orange curves) to the stable Φ^s. At $\kappa \approx -0.712$, two new stable equilibria $\Lambda^{1,2}$ branch off Φ^s in the supercritical pitchfork bifurcation. Unstable manifolds of the saddles detach from Φ^s and instead connect both saddles to each of the newborn steady states [Fig. 4(b)]. Close to the pitchfork, the contour C features two cusps at the steady states, eventually smoothed by further growth of $|\kappa|$ [Fig. 4(c)]. In the next stage, the pair (Σ^1, Λ^1) comes closer, merges and disappears, undergoing a SNIC [Fig. 4(d)]; the same happens to (Σ^2, Λ^2). As a consequence, C forms the orbit of a periodic two-cluster state. Since, in terms of the decrease of κ, the double SNIC occurs after the pitchfork, the periodic orbit in this case is born when Φ^s is already unstable.

Note that whether the pitchfork bifurcation of Φ^s is sub- or supercritical is not a strict indicator for the kind of bifurcation that creates the periodic orbit. While a supercritical pitchfork is necessary for the double SNIC to occur as long as no other steady states (besides Φ^s, Φ^u, $\Sigma^{1,2}$, and $\Lambda^{1,2}$) exist, it is not sufficient. For example, for decreasing κ at $\omega = 0.6$, the orbit flip—transition from double heteroclinic to the double SNIC—occurs at $\epsilon_{\text{flip}} \approx -0.0245$ when the pitchfork of Φ^s is still supercritical. Only for $\epsilon < \epsilon_1 \approx -0.1342$ does the pitchfork of Φ^s become subcritical so that for $\epsilon_1 < \epsilon < \epsilon_{\text{flip}}$ there is a double heteroclinic bifurcation, followed by two simultaneous saddle-node bifurcations of $\Sigma^{1,2}$ with $\Lambda^{1,2}$. At $\epsilon = \epsilon_{\text{flip}}$, both bifurcations coincide, and for $\epsilon > \epsilon_{\text{flip}}$, the periodic orbit emerges through the double SNIC.

Both discussed scenarios, via the double heteroclinic connection and via the double SNIC, have been confirmed for the type of on-site dynamics (3b) as well.

Permutation symmetry, graphically recognizable in Figs. 3 and 4 as reflection invariance of phase portraits with respect to the main diagonal, is inherited by the new periodic trajectory. Symmetry in the phase space translates into the spatiotemporal one: During the oscillation, instantaneous cluster positions are shifted, with respect to each other, by half of the period. Thereby, in the reduced system the oscillation is a splay.

E. Scenarios for unequal cluster sizes

The fact that both discussed bifurcation scenarios involve two simultaneous bifurcations (either heteroclinic or SNIC) clearly is due to the equal sizes of the clusters. The answer to the question what happens for two unequal clusters is, at least for moderate difference in cluster size, that the scenarios are largely similar: Periodic orbits emerge from trajectories, biasymptotic to the equilibria. The pitchfork bifurcation of the synchronous steady state Φ^s is replaced by a transcritical bifurcation [8]; this, however, does not affect the onset of oscillations. There, the main difference is that in the first scenario, there are two global bifurcations, and in the second one, the two SNIC occur one after another; see Figs. 5 and 6 for a system of two clusters of size ratio $p = 2/5$. For the case in Fig. 5, at first the contour C detaches from the saddle Σ^2 via the formation of heteroclinic connection from Σ^1 to Σ^2, and then, after forming the homoclinic loop to Σ^1, it turns into the attracting smooth closed curve. In the unfolding of the double SNIC in Fig. 6, the pair Σ^2 and Λ^2 first vanishes in a SNIC before the same happens to Σ^1 and Λ^1. Note that in both cases the periodic orbit is born at stronger repulsion than under $p = 1/2$, especially in the latter case, while the formation of heteroclinics or SNIC happen at weaker repulsion compared to the symmetric case. This matches the observation from Sec. II C that stronger asymmetry (deviation from $p = 1/2$) requires larger repulsion for periodic orbits to form; see Fig. 2.

F. Stability of two-cluster periodic orbits against splitting

1. General remarks

The reduced system (7) offers full information on whether periodic two-cluster solutions of (1) exist and how they

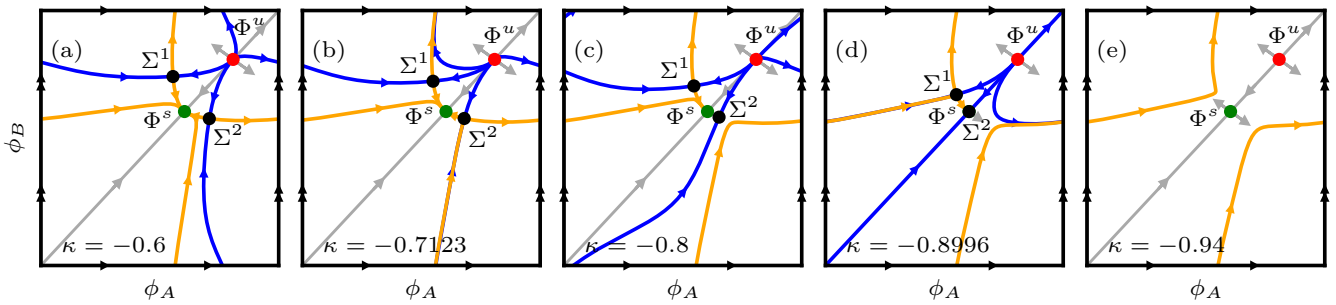

FIG. 5. Stages of bifurcation scenario, creating a periodic two-cluster state (ϕ_A, ϕ_B) with $p = 2/5$ (e.g., in an ensemble of $N = 4 + 6$ units), at $\omega = 0.8$ and $\epsilon = -0.2$ for on-site dynamics of the type (3a). In panel (b), the heteroclinic connection from Σ^1 to Σ^2 is formed. In panel (d), a homoclinic trajectory to Σ^1 is present; its breakup leaves the smooth attracting trajectory [panel (e)].

emerge, but it is of limited use for the question of the asymptotic stability of these states: It characterizes only the perturbations that leave both clusters whole. Perturbations that split one or both of the clusters should be considered in the frame of the full original system.

Periods of oscillatory states, born in the heteroclinic or SNIC bifurcations, are infinite at the bifurcation parameter values. At small deviations from these values, the periods are large, with the dominating portion spent in a slow passage across the immediate vicinity of the saddle point. Hence, right after the bifurcation, stability against splitting is inherited from the parent saddle point: A clustered periodic orbit, branching off the separatrices of the nonsplittable saddle, is stable against splitting perturbations as well. If, on the contrary, the saddle is unstable toward cluster splitting, the newborn periodic orbit is also unstable. Further into the domain of its existence, the orbit spends less time near the saddle and the picture may change; as we will see, this indeed happens.

Asymptotic stability of a periodic solution is determined by its Floquet multipliers: eigenvalues of the monodromy matrix of the orbit. Since instantaneous coordinates inside clusters coincide, this matrix is highly degenerate, its spectrum featuring similar characteristics to the Jacobian of a two-cluster state of rest. Two simple "nonsplitting" multipliers (one being the trivial value 1) determine stability inside the two-cluster subspace. At cluster sizes pN and $N(1-p)$, there are just two "splitting" Floquet multipliers, with multiplicities $pN - 1$ and $N(1-p) - 1$ respectively. On naming these degenerate multipliers after the clusters, affected by the corresponding perturbations, $|\mu^A|$ and $|\mu^B|$, the stability condition becomes $|\mu^A| < 1,\ |\mu^B| < 1$.

For a clustered T-periodic orbit $(\phi_A^0(t), \phi_B^0(t))$, these splitting Floquet multipliers are given by

$$\mu^A = \exp\left(\int_0^T \lambda^A(t)\,dt\right),$$
$$\mu^B = \exp\left(\int_0^T \lambda^B(t)\,dt\right), \tag{12}$$

with the time-dependent versions of (8) and (9):

$$\lambda^A(t) = f'\left(\phi_A^0\right) - \kappa\left(p + (1-p)\cos\left(\phi_B^0 - \phi_A^0\right)\right),$$
$$\lambda^B(t) = f'\left(\phi_B^0\right) - \kappa\left((1-p) + p\cos\left(\phi_A^0 - \phi_B^0\right)\right).$$

If the sizes of clusters A and B coincide, the oscillation, as noted above, is invariant against permutation of A and B. Hence, in that case μ^A and μ^B coincide as well, and all $N-2$ splitting Floquet multipliers are equal.

2. *Stability of equal oscillatory clusters*

We start the discussion of stability of clustered oscillatory states with the case of equal clusters $(p = 1/2)$. Exemplary diagrams in Figs. 7 and 8 refer to on-site dynamics of the type (3a); Fig. 9 characterizes the type (3b). There, blue shaded regions indicate presence of a stable periodic two-cluster state whereas red shading means the existence of an unstable periodic two-cluster state. In the white regions, there are no periodic two-cluster states whatsoever. In each diagram, the green curve marks the transcritical heteroclinic bifurcation

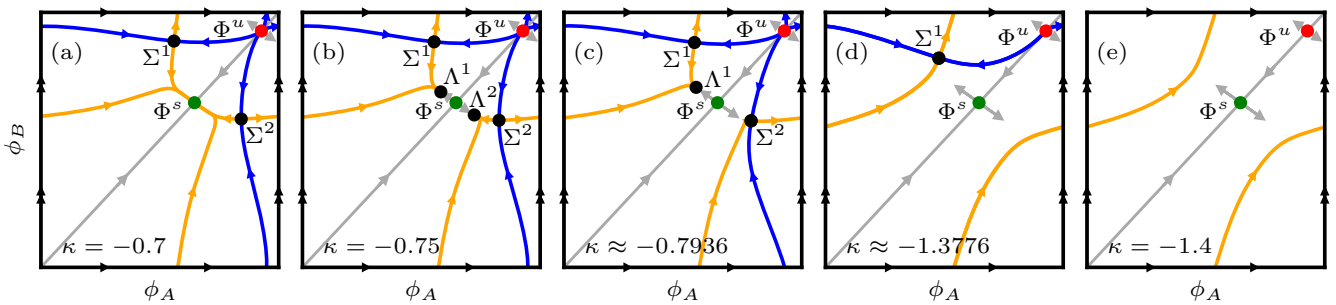

FIG. 6. Stages of SNIC bifurcation scenario, creating a periodic two-cluster state (ϕ_A, ϕ_B) with $p = 2/5$ at $\omega = 0.6$ and $\epsilon = 0.2$ for on-site dynamics of the type (3a). Two SNIC bifurcations of the respective pairs of steady states $\Sigma^{1,2}$ and $\Lambda^{1,2}$ happen at noncoinciding values of κ [panels (c) and (d)].

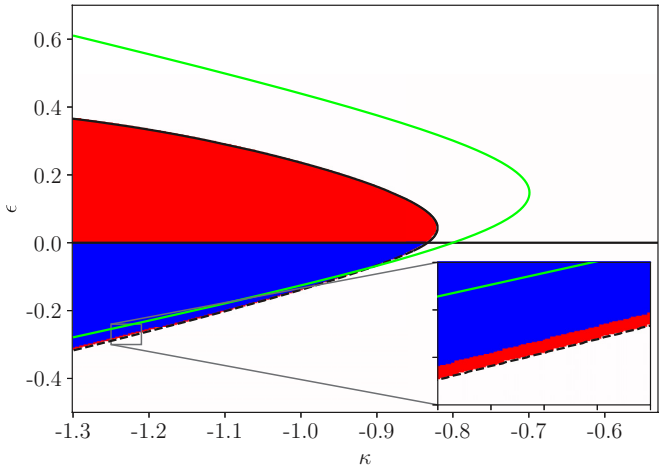

FIG. 7. Existence and stability of periodic oscillations for two equal clusters ($p = 1/2$) with on-site dynamics of the type (3a) at $\omega = 0.6$, in dependence on κ and ϵ. White shading: no periodic two-cluster states exist. Blue (red) shading: asymptotic stability (instability) of the two-cluster periodic state. A switch in stability occurs at $\epsilon = 0$ via WS integrability. At $\omega = 0.6$, periodic solutions are born for $\epsilon < \epsilon_{\text{flip}} \approx -0.0245$ in a double heteroclinic bifurcation (dashed black curve), and for $\epsilon > \epsilon_{\text{flip}}$ in a double SNIC (solid black curve). Solid green curve: pitchfork bifurcation of the synchronous state of rest Φ^s, subcritical for $\epsilon < \epsilon_1 \approx -0.13429$ and supercritical for $\epsilon > \epsilon_1$. The inset shows that for negative ϵ the new oscillatory state is unstable as well; it gets stabilized only at some distance from its creation.

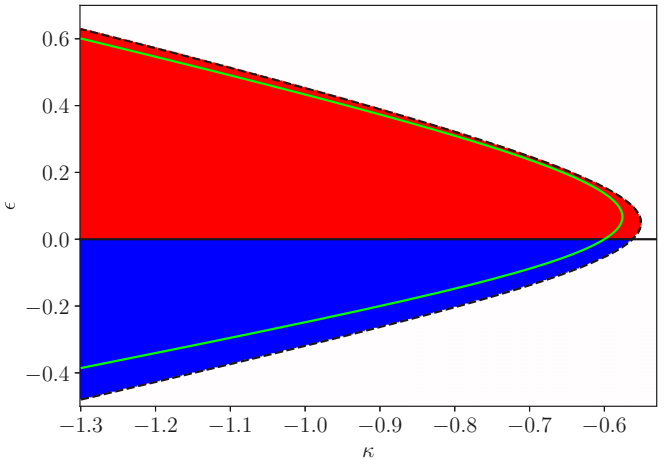

FIG. 8. Existence and stability of periodic oscillations for two equal clusters ($p = 1/2$) with on-site dynamics of the type (3a) at $\omega = 0.8$ in dependence on κ and ϵ. White shading: no periodic two-cluster states exist. Blue (red) shading: asymptotic stability (instability) of the two-cluster periodic state. A switch in stability occurs at $\epsilon = 0$ via WS integrability of the system. The green curve marks the pitchfork bifurcation of Φ^s. When periodic solutions are born in the double heteroclinic bifurcation (dashed line), the state of rest Φ^s is still stable.

(THB) of the synchronous equilibrium Φ^s [8], that involves the pitchfork bifurcation, discussed in Sec. II D. Solid black curves denote the double SNIC while dashed black curves mark the double heteroclinic bifurcation.

In the diagrams, the right border of the existence domain of the two-cluster periodic orbits distinctly does not coincide with the THB which destabilizes Φ^s. This puts two-cluster oscillations in contrast to the splay states which, as we show elsewhere [18], are created in the THB.

The intersection, close to $\epsilon \approx -0.09$ and $\kappa \approx -0.91$ in Fig. 7, of the solid green curve of the pitchfork bifurcation with the dashed curve of the double heteroclinic connection between the saddles $\Sigma^{1,2}$ is merely a projection artifact, not a bifurcation point of higher codimension: in the phase space, the pitchfork and the double heteroclinic connection occur at distant positions.

The diagrams include regions of bistability: The stable periodic oscillation of two equal clusters can coexist either with the attracting synchronous state of rest Φ^s (if the double heteroclinic bifurcation precedes the pitchfork of Φ^s, and the newborn periodic orbit is stable, like in Figs. 7–9 for $\epsilon < 0$) or, in case of the supercritical pitchfork of Φ^s, with the stable equilibria $\Lambda^{1,2}$ (e.g., for $\omega = 0.6$, $\epsilon = -0.95$, and $\kappa = -0.96$).

A common property of all three diagrams is the change of stability exactly at $\epsilon = 0$: Clustered oscillations are unstable at positive values of ϵ and stable in the large part of the region $\epsilon < 0$. The only exception at negative ϵ is an additional narrow instability region in the immediate vicinity of the heteroclinic bifurcation at κ_{het}: At $\omega = 0.6$, this region, whose width shrinks to zero for $\epsilon \to 0$, is shown in the inset of Fig. 7; at $\omega = 0.8$, it is too narrow to be resolved graphically. A further decrease of κ brings stabilization with respect to splitting perturbations.

The periodic splay states, as well as the clustered splay states, are not shown in these diagrams; they exist to the left

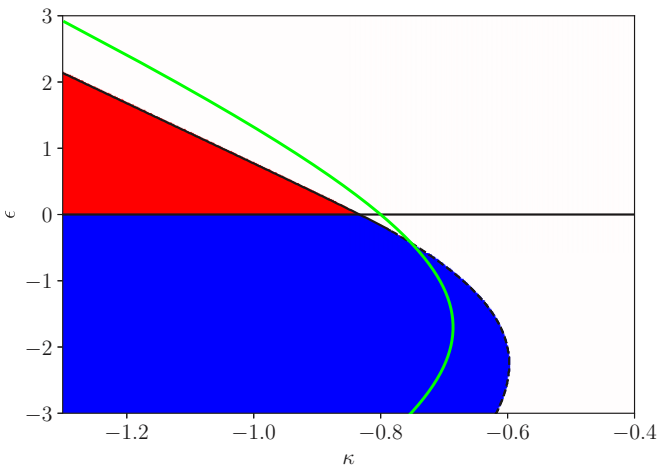

FIG. 9. Existence and stability of periodic oscillations for two equal clusters ($p = 1/2$) with on-site dynamics of the type (3b) at $\omega = 0.6$ in dependence on κ and ϵ. White shading: no periodic two-cluster states exist. Blue (red) shading: asymptotic stability (instability) of the two-cluster periodic state. Periodic solutions are born either in double heteroclinic bifurcations for $\epsilon < \epsilon_{\text{flip}} \approx -0.245$ (dashed black curve) or in a double SNIC for $\epsilon > \epsilon_{\text{flip}}$ (solid black curve). A switch in stability via WS integrability occurs at $\epsilon = 0$. Green curve: the pitchfork bifurcation of Φ^s.

of the green lines of the pitchfork bifurcation. In contrast to the periodic two-clusters, the splay formations, according to numerics, are unstable for negative values of ϵ, whereas some of them are stable at positive ϵ. Therefore, the line $\epsilon = 0$ marks the transfer of stability between two kinds of collective oscillations: Two equal clusters versus the splay or clustered splay. Stability exchange is nonlocal: In the phase space two-cluster states and the splay formations stay separated by finite distances.

Unusual nonlocality of the stability switch owes to the fact that at $\epsilon = 0$ and $\kappa < \kappa_0$ (that is, after the transcritical heteroclinic bifurcation of Φ^s) the families (3a) and (3b) belong to the WS class. The phase space of a system from this class contains a continuum of trajectories with $N-3$ zero Lyapunov exponents [16]; for every periodic orbit this implies $N-3$ Floquet multipliers equal to 1. For each of these orbits, $N-3$ constants of motion are cross ratios between the complex numbers $z_j = \exp(\mathrm{i}\phi_j)$ [16,17]. In fact, a periodic solution with two equal clusters possesses $N-2$ unit multipliers: half of them ensures neutrality with respect to splitting of one cluster, whereas another half refers to splitting of another one. Globally, at $\epsilon = 0$ both the periodic states with equal clusters and the splay formations are embedded in the continuum of neutrally stable solutions, and stability is "instantaneously transferred" along this continuum from the latter to the former.

Remarkably, the periodic two-cluster state at $\epsilon = 0$ can also exist when the repulsion is weaker than the critical threshold, that is, at $\kappa > \kappa_0$: before the destabilization of the synchronous state of rest Φ^s in the course of the THB. In that range of κ, seen, e.g., in Fig. 8 for $\omega = 0.8$, this is the only (up to permutations of the units) periodic solution: There are no further periodic states yet. Therefore, the presence of $N-2$ unit Floquet multipliers for the two-cluster state does not imply existence of the SW continuum of periodic orbits. Within the linearized description, perturbations of the two-cluster oscillatory state stay neutral; nonlinear evolution lets them tend to the equilibrium Φ^s.

For the two-cluster state, the change of stability can be understood by the following argument. Let the cluster A contain, among others, the phases ϕ_1 and ϕ_2 and cluster B contain the phases ϕ_{N-1} and ϕ_N. Since $\phi_A \neq \phi_B \ \forall t$, the cross ratio (CR)

$$\mathrm{CR}_{1,2,N-1,N} = \frac{(z_1 - z_2)(z_{N-1} - z_N)}{(z_1 - z_N)(z_{N-1} - z_2)} \tag{13}$$

is well defined in an open neighborhood of the periodic state and additionally is a constant of motion for $\epsilon = 0$ due to WS integrability. Take an initial state on the clustered orbit, with instantaneous cluster coordinates (ϕ_A, ϕ_B). For a perturbation $(\delta, -\delta, 0, \ldots, 0, \delta, -\delta)$, the cross ratio (13) equals

$$\frac{2\sin^2\delta}{\cos(\phi_A - \phi_B) - \cos 2\delta}.$$

For a small $|\delta|$, after the period T, the linearized evolution transforms the perturbation into $(\mu^A\delta, -\mu^A\delta, 0, \ldots, 0, \mu^B\delta, -\mu^B\delta)$, whereas the cross ratio of the perturbed orbit becomes

$$\frac{2\sin(\mu^A\delta)\sin(\mu^B\delta)}{\cos(\phi_A - \phi_B) - \cos(\mu^A\delta + \mu^B\delta)}.$$

Coincidence, regardless of (ϕ_A, ϕ_B), of both values of the cross ratio at zero ϵ and small $|\delta|$ yields the condition $\mu^A\mu^B = 1$. Due to the permutation invariance of the clusters, both multipliers are equal, rendering $(\mu^A)^2 = 1$. The multipliers are positive (otherwise the perturbation must vanish somewhere on the orbit), and therefore $\mu^A = 1$.

For systems governed by (2), the monodromy matrix (and hence its eigenvalues) depends continuously on the system parameters, in particular on ϵ. According to numerical evidence, at $\epsilon = 0$ the Floquet multipliers cross the critical value 1 transversely: There seems to be no mechanism for additional degeneracies like nontransversality. As a result, at $\epsilon = 0$ there is a compulsory change of stability for periodic solutions with two equal clusters. For clustered states, $N-2$ Floquet multipliers cross the value 1 from above; for the splay states, the multipliers move in the opposite direction. This stability reversal at $\epsilon = 0$ is common in one-parameter families crossing the WS class.

For small nonzero values of ϵ, the cross ratios turn from constants of motion into slowly evolving variables. Locally, velocity of the slow motion in the phase space depends on the sign of ϵ. In particular, near the two-clustered periodic orbit, the motion is directed toward this orbit for $\epsilon < 0$ and away from it for $\epsilon > 0$.

At $\epsilon > 0$, when the periodic two-cluster state is unstable, a perturbation slowly explores the landscape near the invariant manifold that formerly comprised the continuum of periodic orbits, until reaching a new attractor, which is usually a (clustered) splay state. Sometimes simulations disclose attractors that are not perfect clustered splay states: Clusters may vary in size. As an example, a small perturbation of the periodic two-cluster state in the ensemble of 200 active rotators may, depending on its initial configuration, evolve, toward a clustered splay state of four clusters with 50 units in each of them, or toward a state of four clusters with 49, 49, 51, and 51 units. Numerics confirms that at larger N dispersion of cluster sizes in these (almost) clustered splay states wanes: the larger N, the closer to each other in size are the single clusters. Notably, while clustered splay states with high numbers of clusters formally exist for large N, numerical tests for weakly perturbed two-cluster states mostly end up at those with $\leqslant 10$ clusters.

3. Stability for nonequal oscillatory clusters

When the sizes of the oscillating clusters differ, the argument about the invariance, at $\epsilon = 0$, of the cross section for the perturbed clustered periodic orbit remains valid and implies that the product of two splitting Floquet multipliers equals 1. This notable identity holds for all WS-integrable systems with periodic two-cluster states[4] and matches a similar finding for a system of Kuramoto-Sakaguchi oscillators under common multiplicative noise [39]. However, without the permutation symmetry between the clusters, the Floquet multipliers are not

[4]This does not imply, however, conservation of the phase volume near the periodic orbit: For nonequal clusters, the Floquet multipliers have different multiplicities.

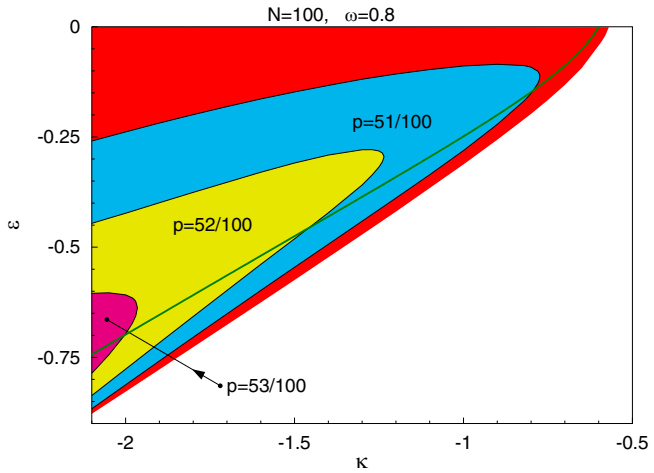

FIG. 10. Existence and stability of periodic oscillations for two unequal clusters with on-site dynamics of the type (3a) at $\omega = 0.8$. Ensemble size $N = 100$. White shading: no oscillating unequal clusters exist. Red shading: oscillating unequal clusters exist but are unstable toward splitting. Blue shading: stable oscillation of two unequal clusters with $p = 51/100$. Yellow shading: coexistence of stable oscillations for clusters with $p = 51/100$ and $p = 52/100$. Magenta shading: coexistence of three stable oscillatory states with, respectively, $p = 51/100$, $p = 52/100$, and $p = 53/100$. Green curve: transcritical bifurcation of Φ^s.

equal. The multiplier governing the stability of the larger cluster exceeds 1; the multiplier responsible for the integrity of the smaller cluster is, on the contrary, smaller than 1: Distant units from the larger cluster hold the smaller one together by their repelling force.

As a result, periodic solutions with two clusters of nonequal sizes feature in the WS case $\epsilon = 0$ a remarkable distinction: Unlike the other periodic orbits, they are not embedded in the $(N-3)$-dimensional continuum of neutrally stable orbits, but are robust isolated phase trajectories. These solutions are unstable toward perturbations splitting the larger cluster [39]. Since the corresponding Floquet multipliers are separated from 1, this effectively rules out a possibility of such states as eventual attractors for sufficiently small $|\epsilon|$. However, at small negative values of ϵ, the larger Floquet multiplier decreases, opening possibilities for stabilization, so that the stronger deviations from the WS case enable stable oscillations of two unequal clusters.

Figure 10 shows on the parameter plane the domains of stability for an ensemble of $N = 100$ units with slight mismatches in the sizes of two clusters. A nested pattern of the stability regions ensures multistability: Regions for larger deviations of p from $1/2$ lie inside similar regions for smaller deviations. Besides, these stable states coexist with periodic oscillations of two equal clusters (cf. Fig. 8) and (below the green curve) with the stable state of rest. Here, we again observe the tendency, noted while discussing the existence domains of unequal clusters in the parameter space: the further the value of p from $1/2$ (i.e., the larger the relative mismatch between the cluster sizes), the stronger should be the repulsion and the bigger the deviation from the WS case $\epsilon = 0$, in order to stabilize the clustered oscillation.

TABLE I. Chosen parameters for Eq. (14), yielding class I excitability, according to Refs. [25] and [26].[a]

Parameter	Ermentrout and Kopell	Tsumoto *et al.*
C	1	1
λ_0	0.33	1/3
g_{Ca}	1	4
V_{Ca}	1	1
g_{L}	0.5	2
V_{L}	0.4	0.5
g_{K}	2	8
V_{K}	0.7	2/3
V_a	−0.01	−0.01
V_b	0.15	0.15
V_c	0.1	0.1
V_d	0.145	0.145
I_{app}[b]	0.0332	395/1200

[a]For the values in Ref. [26], we rescale V in such a way that $V_{\mathrm{Ca}} = 1$, and C and t so that $C = 1$ and $\lambda_0 = 1/3$.
[b]The parameter I is free in Ref. [26] and fixed in Ref. [25]. We choose the shown values to bring the single neuron closer to its SNIC.

III. COUPLED MORRIS-LECAR NEURONS

For a look at existence and stability of periodic two-cluster states in ensembles of class-I excitable units with individual dynamics of dimension higher than 1, we take a set of coupled Morris-Lecar neurons [24]. This conductance-based neuron model was originally designed to describe the neurophysiological properties of the barnacle giant muscle fiber. Its variables are the membrane voltage V of a neuron and the slow recovery variable w that mimics the normalized conductance through the cell membrane for K^+ ions and instantaneous normalized conductance for Ca^{2+} ions. In a region of its parameter space, the model displays class I excitability. A typical setting in this context (see, e.g., Refs. [6,7]) involves a group of N such neurons and assumes that they are all-to-all coupled via their mutual voltage differences:

$$C\dot{V}_i = g_{\mathrm{Ca}}\, n_\infty(V_i)(V_{\mathrm{Ca}} - V_i) - g_{\mathrm{K}}\, w_i(V_{\mathrm{K}} + V_i) - g_{\mathrm{L}}(V_{\mathrm{L}} + V_i) + I_{\mathrm{app}} + \frac{\kappa}{N}\sum_{j=1}^{N}(V_j - V_i), \quad (14a)$$

$$\dot{w}_i = \lambda(V_i)[w_\infty(V_i) - w_i], \quad (14b)$$

where j denotes the jth neuron, the functions $n_\infty(V) = \frac{1}{2}(1 + \tanh\frac{V-V_a}{V_b})$ and $w_\infty(V) = \frac{1}{2}(1 + \tanh\frac{V-V_c}{V_d})$ characterize the proportion of open ion channels for the Ca^{2+} and K^+ ions, and $\lambda(V) = \lambda_0 \cosh\frac{V-V_c}{V_d}$ is the V-dependent inverse recovery time for the K^+ channels.[5] The coefficients $(g_{\mathrm{Ca}}, g_{\mathrm{K}}, g_{\mathrm{L}})$ and $(V_{\mathrm{Ca}}, V_{\mathrm{K}}, V_{\mathrm{L}})$ denote, respectively, the conductances and the reversal potentials, $V_{a,\ldots,d}$ are auxiliary constants, and, finally, I_{app} is the external current. The original model (uncoupled single unit) features a variety of intrinsic dynamics, depending on the choice of system parameters. On

[5]In Ref. [26], $\lambda(V) = \lambda_0 \cosh\frac{V-V_c}{2V_d}$. We use this function for parameters from that reference.

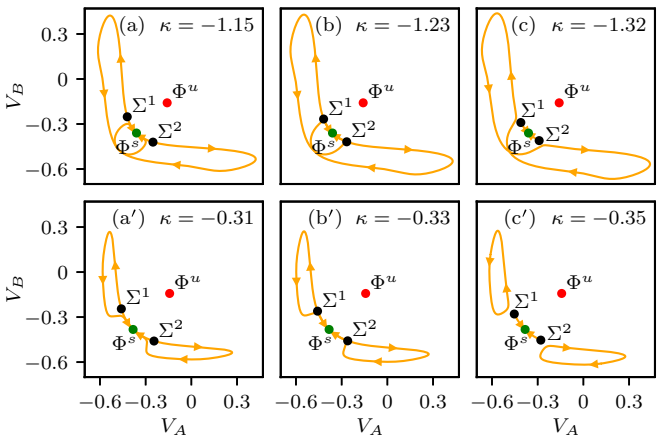

FIG. 11. Bifurcation scenarios for an ensemble of Morris-Lecar neurons that lead to two equally sized oscillating clusters. $\Phi^{s,u}$, synchronous states of rest; $\Sigma^{1,2}$, saddle equilibria. In the top row, system parameters are chosen according to Ref. [26] but with $I_{\text{app}} = 7/30$ for a better resolution of the depicted orbits. From panels (a) to (c), coupling κ gradually becomes more repulsive, resulting at $\kappa \approx -1.23$ in onset of time dependence via the double heteroclinic bifurcation, like in the phase model. In the bottom row, system parameters are chosen according to Ref. [25], but with $I_{\text{app}} = 0$ for better optics. Since I_{app} is chosen sufficiently far from the SNIC of the single neurons, the transition from (a′) to (c′) involves two simultaneous homoclinic bifurcations at $\kappa \approx -0.33$, leaving two periodic two-cluster orbits; for each orbit one cluster is spiking while the other performs weak subthreshold oscillations.

taking the parameter values from Table I, the system gets close to the SNIC [25,26]. Note that the two choices of parameters differ essentially in the scaling of the conductances: The conductances in Ref. [26] are four times higher than in Ref. [25]. Although the current I_{app} is significantly different for the two cases, an expansion of (14a) in powers of V_i renders very similar ratios of the zeroth- to first-order terms, since those depend on the conductances as well. A suitable rescaling of the V_i then eliminates I_{app} and leads to the form $\dot{V}_i = -c + V_i + \cdots$, where the constant $c > 0$ is roughly the same for both choices of parameters. Since I_{app} only enters the zeroth-order term and thus c, the two choices of parameters indeed only differ significantly in their respective conductances. In analogy to our phase equations, varying the scaling of g_{Ca}, g_{L}, and g_{K} thus acts in the same way as changing the parameter ϵ in (2) while keeping ω approximately constant. The sign of κ again determines whether coupling is attractive ($\kappa > 0$) or repulsive ($\kappa < 0$), the difference to the phase model being that it acts in the voltage variables and is linear.

Again, we focus on existence and stability of periodic two-cluster solutions of (14) for repulsive coupling.

Like in the ensemble of active rotators, there is a synchronous state of rest that undergoes the transcritical bifurcation at a critical value of κ. Here, as well, periodic two-cluster states can emerge not via this transcritical bifurcation but through double heteroclinic bifurcations of two two-cluster saddle points; see, for example, the top row in Fig. 11. Again, we choose clusters of equal size: $p = 1/2$. The top row shows the creation of a periodic orbit from the heteroclinic contour, similar to the one found for the ensemble of phase variables. Starting in Fig. 11(a) with κ above the bifurcation value $\kappa_0 \approx -1.23$, two pairs of separatrices connect the saddle equilibria with the stable state of rest. At $\kappa = \kappa_0$, the separatrices form two heteroclinic connections between the saddles [Fig. 11(b)]. Finally, for $\kappa < \kappa_0$ there is a single periodic two-cluster state where both clusters perform large-scale oscillations in antiphase [Fig. 11(c)].

Remarkably, taking the parameters from Ref. [26] but choosing the current I_{app} below the critical value $I_0 \approx 0.03264$ leads to a different scenario, where not the unique periodic two-cluster state, but two distinct periodic states emerge: See the bottom row of Fig. 11. There, the separatrices, shown in Fig. 11(a′), form in Fig. 11(b′) not heteroclinic connections but two simultaneous *homoclinic* loops from which two separate periodic orbits emerge [Fig. 11(c′)]. On each of the latter, one of the clusters performs a large scale "spiking" oscillation while the other cluster displays only weak "subthreshold" vacillation near the state of rest. Compared to the phase model described above, this "chimera-like" splitting in two populations with different spiking properties is a different kind of dynamics.

Regarding the stability of the periodic two-cluster states with respect to splitting, we find that, e.g., for an ensemble of $N = 20$ neurons with the parameters from Ref. [26], the orbit is stable close to the bifurcation ($\kappa_0 \approx -0.2$) while for the parameters from Ref. [25] ($\kappa_0 \approx -0.024$) it is unstable. This further justifies the interpretation of the conductance scaling as an analog of the parameter ϵ. In the second case, small perturbations of the unstable orbit grow and eventually converge either to the still stable Φ^s or, if $|\kappa|$ is sufficiently large to destabilize Φ^s, toward a (pure) splay state. This notable similarity to the picture of stability for two-cluster and splay states found in the phase model hints that the interplay between the stability of splay and two-cluster states may be a more general feature for systems of (identical) class I excitable units.

IV. CONCLUSIONS

Ensembles of identical one-dimensional class I excitable units feature nontrivial dynamics only for repulsive coupling. Two widespread modes of collective oscillations occurring in this context are splay states and two-cluster states. We have investigated how the latter emerge through two different types of global bifurcation scenarios, focusing on states with two clusters of equal size. One type is a double SNIC where, on an invariant curve, two pairs of two-cluster saddle steady states simultaneously vanish, transforming thereby the curve into a periodic orbit. The second type is a bifurcation in which a periodic solution is born from the pair of heteroclinic trajectories that connect two-cluster saddles. According to Ref. [35], this scenario should be typical in situations where each of the single units, if decoupled, is sufficiently close to the SNIC.

For a system of active rotators, stability of periodic states with two clusters of equal size is directly linked to the higher Fourier modes of on-site dynamics. In the presented case, a change of the sign of all higher order Fourier terms in the equations of motion results in the stability reversal.

In general, two stable oscillating clusters may differ in their sizes. For a given ensemble size, the stability regions in the parameter space for solutions with larger difference between

the cluster sizes are nested inside the analogous regions for solutions with smaller size mismatch.

To view our findings in a more general context, we have also briefly discussed an ensemble of coupled two-dimensional class I excitable units: the Morris-Lecar neurons. For them, the double heteroclinic connection has been verified as a mechanism for the creation of two-cluster oscillations. Stability of the resulting states with respect to perturbations splitting the clusters depends on the values of the system parameters. Notably, in the case where the oscillatory two-cluster states are unstable, we, like in the phase model, find instead a stable splay state. This looks intriguing since the splay states and the two-cluster states have their origin in quite different bifurcation scenarios. Interconnections between splay states and two-cluster oscillatory states will be a subject of a future work.

Of course, ensembles of completely identical units are idealizations, and the effect of introducing slight heterogeneity into the ensemble is of legitimate interest. Outside of bifurcations, the described periodic states are structurally stable, and a sufficiently weak heterogeneity can neither destroy nor destabilize them. Exact coincidence of coordinates inside each cluster will be replaced by formation of "imperfect clusters": tightly grouped sets of coordinate values. Transformation of bifurcation scenarios is less straightforward: robustness of heteroclinic orbits often relies heavily on the permutation symmetry among the units [40]. Since weak heterogeneity would not change the dimension of invariant manifolds of the saddle steady states, similar sequences of nonsimultaneous global bifurcations like in Sec. II E should be expected. The same arguments should ensure persistence of bifurcation scenarios in the case when sufficiently small higher order terms are included into the coupling function. Yet another possibility to lower the degree of symmetry in the system is to diversify the contributions of different units into the common global field, e.g., to replace in the coupling term of Eq. (1) the uniform coupling strength κ by summation over the individual coupling strengths κ_j of the units. Preservation, at $\epsilon = 0$, of the WS character of dynamics does not demand all units to be repelling (with all $\kappa_j < 0$); what matters is the sign of the overall sum $\sum_{j=1}^{N} \kappa_j$ [8]. Accordingly, at $\epsilon \neq 0$ the evolution of collective oscillations, including the two-clustered states, should involve bifurcation scenarios, described in the preceding sections.

The discussed periodic solutions are not necessarily the only possible states, let alone attractors. In numerical simulations of the phase model, we encountered examples when perturbations of unstable two-cluster states converged not to a perfect (clustered) splay state but instead to a state that might be called an imperfect clustered splay, where different clusters, while still roughly stacked equally in time, are of different sizes. In models of higher dimension, like the Morris-Lecar model, certain stable periodic states are hardly compatible with the phase model; in an example, two single neurons are spiking in antiphase while the remaining ensemble stays relatively close to the unstable synchronous state of rest, so that the two spiking neurons act as "shepherds" that keep the flock of other neurons in place. For larger N, however, such intricate periodic states seem to become increasingly rare to reach from generic initial conditions. In this sense, two-clusters and (clustered) splay states appear to be most common asymptotic states.

ACKNOWLEDGMENTS

This work has been performed within the scope of the IRTG 1740/TRP 2015/50122-0 and funded by the DFG and FAPESP.

APPENDIX A: EXPRESSIONS FOR THE BIFURCATION CURVES OF THE SYNCHRONOUS EQUILIBRIUM Φ^s

To derive explicit expressions that interrelate parameters at the bifurcations of the synchronous state of rest Φ^s in the reduced system, Eqs. (7), along with bifurcation conditions, are transformed with the help of the Weierstrass (tangent half-angle) substitution

$$\psi \equiv \tan\frac{\phi}{2}, \quad \sin\phi = \frac{2\psi}{1+\psi^2}, \quad \cos\phi = \frac{1-\psi^2}{1+\psi^2}$$

to the form, polynomial in ψ. Bifurcational relations like (4) and (6) are then obtained from the resultants of the corresponding polynomials. Their counterparts for the on-site dynamics of the type (3b) have been derived as well, but are far too long to be cited here explicitly.

APPENDIX B: CRITERION OF CRITICALITY FOR THE PITCHFORK BIFURCATION OF Φ^s

Whether the pitchfork bifurcation of Φ^s at κ_0 for the reduced system

$$\begin{aligned}\dot\phi_A &= \omega - \sin\phi_A + \epsilon\sin 2\phi_A + \frac{\kappa}{2}\sin(\phi_B - \phi_A),\\ \dot\phi_B &= \omega - \sin\phi_B + \epsilon\sin 2\phi_B + \frac{\kappa}{2}\sin(\phi_A - \phi_B)\end{aligned} \tag{B1}$$

is sub- or supercritical depends on the values of parameters ω and ϵ. In the coordinates $x = (\phi_A - \phi_B)/2$ and $y = (\phi_A + \phi_B)/2$, permutation invariance of (B1) translates to mirror symmetry along the y axis:

$$\begin{aligned}\dot x &= f(x,y),\\ \dot y &= g(x,y),\end{aligned}$$

with

$$\begin{aligned}f(x,y) = &-\frac{1}{2}[\sin(x+y)+\sin(x-y)]\\ &+\frac{\epsilon}{2}[\sin 2(x+y)+\sin 2(x-y)]\\ &-\frac{\kappa}{2}\sin 2x,\\ g(x,y) = &\ \omega - \frac{1}{2}[\sin(x+y)-\sin(x-y)]\\ &+\frac{\epsilon}{2}[\sin 2(x+y)-\sin 2(x-y)].\end{aligned}$$

The x-nullcline $y_x(x)$ and y-nullcline $y_y(x)$ are defined by $0 = f(x, y_x(x))$ and $0 = g(x, y_y(x))$, respectively. The trivial branch $x = 0$ of the x-nullcline corresponds to the invariance

of the diagonal $\phi_A = \phi_B$ under the flow of (B1) and can be factored out by considering the solution of $0 = f(x, y_x(x))/x$. Mirror symmetry implies that the nullclines are even functions of x:

$$y_x(x) = a_x + \tfrac{1}{2}b_x x^2 + \mathcal{O}(x^4),$$
$$y_y(x) = a_y + \tfrac{1}{2}b_y x^2 + \mathcal{O}(x^4). \tag{B2}$$

Equilibria of the system correspond to intersections of the nullclines. To determine whether the pitchfork is sub- or supercritical, we make use of the simple geometric consideration: Two parabolas $y_1(x) = a_1 + b_1 x^2$ and $y_2(x) = a_2 + b_2 x^2$ with (i) $b_1 > b_2 > 0$ or (ii) $0 > b_1 > b_2$ intersect if and only if $a_1 < a_2$.

With this observation in mind, we determine criticality of the pitchfork bifurcation. The bifurcation itself is, in these terms, given by the condition $a_x = a_y = \phi^s$, where ϕ^s, as above, denotes the position of the stable steady equilibrium for the single rotator.

Substituting (B2) into the nullcline equations and expanding them to the second order in x, we arrive at

$$b_y = \frac{\sin\phi^s - 4\epsilon\sin 2\phi^s}{\cos\phi^s - 2\epsilon\cos 2\phi^s} \tag{B3}$$

and

$$b_x = \frac{\cos\phi^s}{\sin\phi^s - 4\epsilon\sin 2\phi^s}. \tag{B4}$$

The bifurcation type is determined by the ratio

$$c(\omega,\epsilon) \equiv \frac{b_y}{b_x} = \frac{(\sin\phi^s - 4\epsilon\sin 2\phi^s)^2}{\cos\phi^s(\cos\phi^s - 2\epsilon\cos 2\phi^s)}. \tag{B5}$$

The pitchfork is subcritical if $c(\omega,\epsilon) > 1$ and supercritical if $c(\omega,\epsilon) < 1$. Change of the character of the pitchfork bifurcation occurs at $b_x = b_y$, i.e., $c(\omega,\epsilon) = 1$.

[1] Y. Kuramoto, *Chemical Oscillations, Waves, and Turbulence* (Springer-Verlag, Berlin, 1984).
[2] A. T. Winfree, *The Geometry of Biological Time* (Springer, Berlin, 2001), Vol. 12.
[3] A. Pikovsky, M. Rosenblum, and J. Kurths, *Synchronization* (Cambridge University Press, Cambridge, UK, 2003).
[4] Y. Kuramoto, in *International Symposium on Mathematical Problems in Theoretical Physics*, edited by H. Araki, Lecture Notes in Physics, Vol. 39 (Springer, Berlin, Heidelberg, 1975), pp. 420–422.
[5] I. G. Malkin, *Theory of Stability of Motion*, Vol. 3352 (U.S. Atomic Energy Commission, Office of Technical Information, Washington, D.C., 1959).
[6] D. Pazó and E. Montbrió, Phys. Rev. E **73**, 055202(R) (2006).
[7] H. Daido, A. Kasama, and K. Nishio, Phys. Rev. E **88**, 052907 (2013).
[8] M. A. Zaks and P. Tomov, Phys. Rev. E **93**, 020201(R) (2016).
[9] J. Keener and J. Sneyd, *Mathematical Physiology* (Springer, Berlin, 1998).
[10] E. M. Izhikevich, *Dynamical Systems in Neuroscience* (MIT Press, Cambridge, MA, 2010).
[11] A. Hodgkin, J. Physiol. **107**, 165 (1948).
[12] Y. A. Kuznetsov, *Elements of Applied Bifurcation Theory*, Applied Math. Sciences, Vol. 112 (Springer, Berlin, 2013).
[13] S. Shinomoto and Y. Kuramoto, Prog. Theor. Phys. **75**, 1105 (1986).
[14] R. Adler, Proc. IRE **34**, 351 (1946).
[15] E. Teichmann and M. Rosenblum, Chaos **29**, 093124 (2019).
[16] S. Watanabe and S. H. Strogatz, Physica D **74**, 197 (1994).
[17] S. A. Marvel, R. E. Mirollo, and S. H. Strogatz, Chaos **19**, 043104 (2009).
[18] R. Ronge, M. Zaks, and T. Pereira, Existence and persistence of splay states in a system of active rotators (unpublished).
[19] D. Hansel, G. Mato, and C. Meunier, Phys. Rev. E **48**, 3470 (1993).
[20] L. Lücken and S. Yanchuk, Physica D **241**, 350 (2012).
[21] I. Z. Kiss, Y. Zhai, and J. L. Hudson, Prog. Theor. Phys. Suppl. **161**, 99 (2006).
[22] L. Schmidt and K. Krischer, Phys. Rev. E **90**, 042911 (2014).
[23] F. P. Kemeth, S. W. Haugland, and K. Krischer, Chaos **29**, 023107 (2019).
[24] C. Morris and H. Lecar, Biophys. J. **35**, 193 (1981).
[25] G. Ermentrout and N. Kopell, SIAM J. Appl. Math. **50**, 125 (1990).
[26] K. Tsumoto, H. Kitajima, T. Yoshinaga, K. Aihara, and H. Kawakami, Neurocomputing **69**, 293 (2006).
[27] C. Kurrer and K. Schulten, Phys. Rev. E **51**, 6213 (1995).
[28] M. A. Zaks, A. B. Neiman, S. Feistel, and L. Schimansky-Geier, Phys. Rev. E **68**, 066206 (2003).
[29] C. J. Tessone, A. Scire, R. Toral, and P. Colet, Phys. Rev. E **75**, 016203 (2007).
[30] J. R. Engelbrecht and R. Mirollo, Chaos **24**, 013114 (2014).
[31] P. Ashwin, G. Orosz, J. Wordsworth, and S. Townley, SIAM J. Appl. Dyn. Syst. **6**, 728 (2007).
[32] P. Ashwin, O. Burylko, and Y. Maistrenko, Physica D **237**, 454 (2008).
[33] P. Ashwin, G. King, and J. W. Swift, Nonlinearity **3**, 585 (1990).
[34] P. Ashwin and J. W. Swift, J. Nonlinear Sci. **2**, 69 (1992).
[35] C. Baesens and R. S. MacKay, Nonlinearity **26**, 3043 (2013).
[36] K. Okuda, Physica D **63**, 424 (1993).
[37] O. Popovych, A. Pikovsky, and Y. Maistrenko, Physica D **168**, 106 (2002).
[38] N. Fenichel and J. Moser, Indiana Univ. Math. J. **21**, 193 (1971).
[39] C. C. Gong, C. Zheng, R. Toenjes, and A. Pikovsky, Chaos **29**, 033127 (2019).
[40] M. Krupa, J. Nonlinear Sci. **7**, 129 (1997).